

Co-regulated timing in music ensembles: a Bayesian listener perspective

Marc Leman

30 Nov. 2020

Ghent University, Department of Musicology, IPEM@Krook, Miriam Makebaplein 1, 9000 Gent, Belgium. Email: marc.leman@ugent.be

Abstract:

Co-regulated timing in a music ensemble can be understood as a dynamic system whose components (i.e., musicians) establish an overall state (of timing) through coordinated action (=co-regulation). An algorithm is proposed in which co-regulated timing is modelled from the perspective of a musician-listener who simulates timing constancy using multivariate latent processes based on Bayesian inference. Global features of these latent processes can be extracted, such as fluctuation and stability. The algorithm's smoothness and regularization parameters are explained and illustrated. The algorithm is then applied to real data, first, a performance of a choir consisting of four singers, then, a dataset containing performances of duet singers (Dell'Anna et al, 2020). It is shown that global features of the latent processes correlate with human subjective estimates of the music ensembles' quality and associated experienced agency. In future work, BListener could serve as perception component of an artificial musician in a music ensemble.

1. Introduction and background

Co-regulated timing in a music ensemble can be understood as a dynamic system whose components (i.e., musicians) establish an overall state (of timing) through coordinated action (=co-regulation). From the viewpoint of a music ensemble as a whole, the capacity for timing rests on different modalities of information exchange (Bishop et al., 2019; Bishop and Goebel, 2020) and corporeal expression (Keller and Appel, 2010, Chang et al. 2019), and it is characterized by typical emergent behavior, such as resilience in response to perturbation (Glowinski et al., 2016, 2017; Hilt et al., 2019). Emergent behavior requires a balancing of underlying components and processes, so that the system can maintain a state of constancy despite fluctuations (Davies, 2016; Changeux, 1999, p. 57). In timing, these regulatory forces are directed towards a particular constancy, otherwise joint music performance would become uncertain and unpredictable, and the performance would perhaps be experienced as a "badly timed" performance. The capacity for timing constancy, obviously, depends on musical skills, rehearsal time, musical complexity, and other confounds such as expression (Cochrane et al., 2013; Fabian et al., 2014, Keller, 2014). Ultimately, the quality of the timing will co-affect emotional experiences (Levitin et al. 2018, Schiavio et al., 2017) and embodied synchronizations (Witek et al., 2014; Burger et al., 2017).

From the viewpoint of a musician within a music ensemble, the capacity for timing rests on each musician's capacity to synchronize, entrain, and socially co-regulate the sound-producing actions in view of joint timing intentions (D'Ausilio et al. 2015; Volpe et al., 2016; Bishop, 2018). For example, when an onset from a musician of my ensemble is perceived

earlier than expected, I can counterbalance this unexpected event. Accordingly, my next onset would be timed in such a way that an assumed joint latent hypothesis about the ensemble's tempo, meter, or expressive rhythmical structuring, can be maintained. Note that the assumed constancy also applies to expressive timing, such as increase and decrease of tempo, because what matters is how a musician's observations of timing fit with constancy assumptions about the ensemble's joint intentional timing.

Co-regulated timing has been assumed to rest on the human sensitivity for isochrony (Ravignani and Madison, 2017). While isochrony is a basis for the emergence of timing patterns at higher temporal levels, known as meter and rhythms (Repp and Su, 2013, Kotz et al. 2018, Scheurich et al., 2020), isochrony may be embedded in rather complex temporal patterns and endowed with non-isochronous pulse structures. Yet, even in those circumstances, timing can afford precise and stable rhythmic performance and entrainment (Frühaufer et al., 2013; Polak et al., 2016), suggesting that timing is based on latent processes capable of handling timing fluctuations. We thereby assume that, in these latent processes, listeners are able to “construct” the parameters of (joint) timing constancy, using perceived traces of timing (e.g., onsets) as produced by the music ensemble.

Latent perception processes can be handled by Bayesian inferences on parameters extracted from observations. As known, the Bayesian viewpoint involves a likelihood (how likely it is that a new temporal event stems from the assumed timing constancy) and a prior (the expected timing constancy in absence of observations), from which a posterior (expected timing constancy given the new temporal event) is inferred. In view of a next onset, the prior is updated by replacing the old prior with the posterior. Bayesian inference (Aitchison and Lengyel, 2017) can be conceived of in terms of neural circuits (Friston et al. 2017), hierarchical circuits (Kanai et al., 2015), homeostatic regulation (Pezzulo et al., 2015), or predictive coding (Koelsch et al., 2019). Vuust and Witek (2014) show how rhythm perception can be conceptualized as an interaction between what is heard (“rhythm”) and the brain’s anticipatory structuring of music (“meter”), using the predictive coding model and its implied Bayesian inference.

As far as we know, understanding the dynamics of co-regulated timing from the viewpoint of an active listener is novel. Thereby, we model the listener as a dynamic linear system equipped with latent processes that capture constancy in timing, in view of the prediction that is necessary for co-acting. Pioneering work in cognitive dynamics (e.g. Haken, 1991; Kelso, 1995; Port and Van Gelder, 1995) has been inspiring for using dynamic systems in musical applications, such as gesture analysis (Demos et al., 2014), simulations of musical expectations (Agres et al., 2018), emotion research (Grimaud and Eerola, 2020), and adaptive digital music synthesis and control (Van Nort and Depalle, 2017), but not for co-regulated timing and listening as far as we know.

The goal of the present paper is to propose and benchmark an algorithm which we call the Bayesian listener algorithm, or BListener for short. BListener can be considered a local component of a global dynamic system for co-regulated timing. It is focused on perception rather than on action. However, perception is modelled from the perspective of acting and therefore, a link with operating components will be rather straightforward, provided that the algorithm is implemented in real-time.

The structure of the paper is as follows. In section 2, we present the BListener algorithm and in section 3 its basic diagnostics. In section 4, we benchmark the algorithm with different datasets, and finally in section 5 the limitations and future perspectives are discussed.

2. The Bayesian listener algorithm

In this section, we define the basic timing concepts, and global analysis measures. Then we describe how the Bayesian listening algorithm works at sample level.

2.1. Basic concepts of co-regulated timing

Our modelling will be framed in terms of discrete events. This framing applies to musical contexts in which onsets can be clearly discerned. Using manual annotations, onset-detection algorithms, or a combination of both, we obtain a one-dimensional array of onset times (in milliseconds) that is used as input to the Bayesian listener algorithm. All other timing concepts, at least of Western music, such as inter-onset-intervals, meter and the tempo, can be based on these onsets (Clarke, 1999; London, 2012).

The recording of a music ensemble using a single microphone might suffice for extracting the onsets. Accordingly, all timing objects are based on representations of successive onsets produced by the music ensemble, regardless of the number of musicians and the musician who produces the onset. Successive onsets define *inter-onset-intervals* (IOIs), or durations of the ensemble's onset-output, and these are conceived as the timing objects from which other timing objects are derived. The algorithm aims at tracking timing objects that express timing constancy.

The timing objects can be categorized as inter-onset observations, inter-onset classes (of constancy), and meter and tempo. We use the prefix IOI to stress the fact that all these objects have a duration that can be traced back to inter-onset-intervals. The *IOI-observations*, or *IOI-observed objects*, result from onset-detection and/or onset-annotation of the music ensemble's recorded musical signal. Given two successive onsets extracted from the signal, the IOI-observed object (with its defined duration) becomes available after the second onset. The *IOI-classes* (of constancy but this explicit reference to constancy will be deleted from now on) stand for IOIs that are inferred from the IOI-observations, and they are used to anticipate future IOI-observations. IOI-classes are thus conceived in terms of latent timing parameters. They exist only as the result of a Bayesian inference about the observed co-regulated timing of the music ensemble. As latent parameter values of a (stochastic) process, IOI-classes will be defined by (Gaussian) distributions, with mean and variance. The mean will define the duration of the IOI-class and the variance will define the uncertainty about this duration. *Multiple IOI-classes* can be tracked in parallel, and as musical time proceeds, this IOI-classes result is a multivariate time series of constancy. Moreover, the Bayesian inference about the IOI-classes can be regularized by a meter, which operates as a hyper-parameter that constraints the variance in the ratio among IOI-classes. That meter is called the *out-of-time IOI-meter*, as it defines an assumed ratio among IOI-classes, disregarding how time evolves. For example, an IOI-meter with ratio {3, 2, 1} represents IOIs having an assumed ideal duration, for example, of 1500, 1000, 500 milliseconds, or, of 600, 400, 200 milliseconds. The IOI-meter can be extracted from a musical score or it can be an assumption about the relationship among IOI-classes, possibly derived from an inspection of data. For example, in an off-line analysis, one could use k-means clustering of the IOIs to obtain an estimate of the out-of-time IOI-meter. The *time-related IOI-meter* defines ratios among the multivariate IOI-

class time series, representing the IOI-class ratio at each sample of the multivariate time series. As shown below, the time-related IOI-meter can be regularized (constrained) by the out-of-time IOI-meter, and this regularization can in turn affect the Bayesian inference about the IOI-classes. Finally, the *IOI-tempo* at a particular moment in time is defined as a linear combination of the IOI-classes at any moment in time, using the out-of-time IOI-meter ratios to calculate a mean of the IOI-class time series. Examples are given below.

Blistener obeys dynamic laws which (for reasons of computational efficiency) will be updated at a sampling rate of 100 samples per second, unless specified otherwise (up to 1000 samples per second). However, inside this dynamic processing, we handle IOI objects in *log2dur scale*. The latter is a log2 transformation of the millisecond scale, and "dur" stands for duration. For example, the relation between 880 and 800 milliseconds is expressed in log2dur as a difference between $\log_2(880)$ and $\log_2(800)$, which is 0.1375 log2dur, and this is the same as the difference between $\log_2(440)$ and $\log_2(400)$, $\log_2(440/400)$ or $\log_2(1.1)$. Many people, however, are used to work with durations in milliseconds rather than in log2dur. Accordingly, if we speak about IOI-meter, we will specify whether the ratio is determined in milliseconds or in log2dur. What counts here is that inside Blistener, IOI objects are all handled in log2dur while the dynamic updating of Blistener proceeds in milliseconds. In the R-package BListener, the above concepts are defined in the function BLmain.

2.2. Global features of co-regulated timing

Global features of the analysis of co-regulated timing are related to fluctuation, stability, narration, and outliers. All these measures somehow involve the IOI-classes. The calculation of fluctuation is based on the prediction error, which is defined as the difference, in log2dur, between the duration of an IOI-observed object and the duration of the IOI-class object at the time when it was assigned to this IOI-class. The mean of the absolute values of all those differences for an IOI-class is the measure *Fluctuation1*, and it is calculated for each IOI-class separately. Alternatively, we take the standard deviation of those differences as another measure of fluctuation, called *Fluctuation2*. The measure *Stability* is obtained by calculating the IOI-class' standard deviation over time.

As IOI-observations get assigned to the IOI-class whose duration is closest, it is possible to label each IOI-observation assignment with a code that represents an IOI-class. Given three IOI-classes, for example, one could thus get a sequence of respective assignments, such as: 1, 2, 1, 3, 2, 2, 3, etc... A measure of entropy or structure can be inferred from it, called Narration. Without going in much detail, we will apply a recurrence analysis (e.g., Nakayama et al., 2020; Tolston et al., 2020) and calculate the recurrence ratio (*RR*), which amounts to a percentage representing structure in terms of the number of points that appear closely together in the phase space versus all points in the phase space, including those that don't appear closely together. Finally, *Outlier* is a measure of outliers, defined as the sum of all IOI-observed durations greater than a specified threshold. Sometimes, outliers can be very small values due to onset mistakes. However, they can also be large, due to a performance breakdown of a few seconds. When detected, outliers are neglected and the system navigates on its own, based on the system's dynamics. In the R-package BListener, these measures are defined in the function BLpost.

2.3. The Bayesian listener algorithm

The Bayesian listener algorithm is described in terms of a state-space model (Petrís et al. 2009; Shumway and Stoffer, 2017), a concept that can be related to a multivariate version of the Kalman filter (cf. Meinhold and Singpurwalla, 1983).

2.3.1. The univariate approach

Figure 1 offers a graphical view of the algorithm at sample level, for the univariate case. The horizontal axis represents discrete time, with black circles as samples at $t-2$, $t-1$, and t . Associated with this time line are instances of one IOI-class (c_{t-2}, c_{t-1}, c_t). The IOI-observed object occurs at o_t . The four small arrows labelled 1 to 4, in Figure 1 show the different steps of a Bayesian inference. While in the multivariate version of the algorithm, Bayesian updating may apply to another IOI-class that runs in parallel, the IOI-observed objects appear in sequence and so, at sample level, Bayesian update is applied to only one IOI-class while the other IOI-classes will be updated according to the system equation, as explained below.

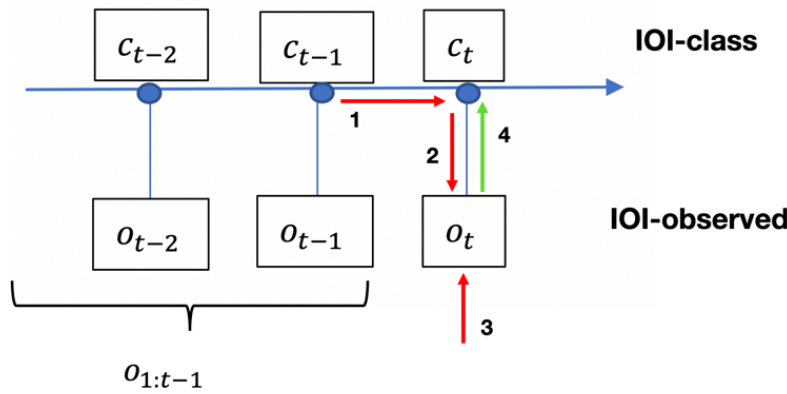


Figure 1. State-space model for Bayesian inference on a single IOI-class

The transition of the IOI-class from one sample to another sample is described by the state equation (Equation 1), while the connection of an IOI-class to the IOI-observation is described by the observation equation (Equation 2). Both equations represent stochastic processes. The label c is used for the IOI-class, and o is used for the IOI-observation. The labels w_t and v_t represent independent noise whose normal distribution is characterized by zero mean and a fixed variance W_t and V_t .

$$c_t = c_{t-1} + v_t \sim N(0, V_t) \quad (\text{Equation 1})$$

$$o_t = F_t c_t + w_t \sim N(0, W_t) \quad (\text{Equation 2})$$

We adopt a simple rule for the state equation (Equation 1), which is that the IOI-class at time t is the same as the IOI-class at time $t - 1$, except that system noise is added. Equation 1 therefore characterizes the stochastic process as *random walk*. Obviously, as the IOI-class is a latent process, its value cannot be directly observed, and thus the goal is to estimate it using IOI-observations that become available.

Provided that the IOI-observation is not an outlier, it is assigned to an IOI-class on the basis of a metric, here: the smallest difference between the duration of the IOI-observed object and the duration of any of the IOI-class objects. After the assignment, the IOI-observed object is handled as an assigned IOI, and Equation 2 applies in order to update the IOI-class using Bayes rule. The noise introduced by Equation 2 accounts for the uncertainty in the observation, such as measurement mistakes in onset detection. While this IOI-observed object is processed (i.e. involving Bayesian inference), the process of the other non-assigned IOI-classes get updated according to Equation 1.

The state equation (Equation 1) and the observation equation (Equation 2) drive stochastic processes that obey Gaussian probability laws. Hence, using the graph of Figure 1, it is possible to specify the steps from one sample to another in terms conditionals:

$$\begin{aligned} c_t | c_{t-1} &\sim N(c_{t-1}, V_t) \\ o_t | c_t &\sim N(F_t c_t, W_t) \end{aligned}$$

The step from c_{t-1} to c_t obeys a Gaussian probability distribution with c_{t-1} as mean and V_t as variance. The step from c_t to o_t obeys a Gaussian probability distribution with $F_t c_t$ as mean and W_t as variance. Both mean and variance follow directly from Equation 1 and Equation 2. The arrows in Figure 1 indicate an updating of the IOI-class, given an IOI-observed object that becomes available. This updating can be understood as a Bayesian inference in three steps.

Step 1 (Prior). Assume that we are standing in position c_{t-1} where we have not yet encountered the IOI-observed object. Given the previously IOI-observed objects up to now (from 1 to $t - 1$), we have a known mean and a known variance of the IOI-class at our disposal, which we denote by: $c_{t-1} | o_{1:t-1} \sim N(\hat{c}_{t-1}, \check{c}_{t-1})$. Note that at the start of the latent process, we just have to make a guess about this mean and variance, denoted \hat{c}_{t-1} and \check{c}_{t-1} . This can be done manually, or by other methods, for example, by k-means clustering on the beginning part of a data-set. Next, we use the state equation (Equation 1) to make a hypothesis (= the prior) about our next IOI-class c_t (see arrow 1): $c_t | o_{1:t-1} = c_{t-1} | o_{1:t-1} \sim N(\hat{c}_{t-1}, \check{c}_{t-1} + V_t)$. Given the conservative approach, our hypothesis about the mean for the IOI-class c_t does not change from our current position and therefore, it has the same mean as the IOI-class c_{t-1} , namely: \hat{c}_{t-1} . The system variance, however, will be the proper variance of the IOI-class that we had, plus the new variance due to system noise, thus $\check{c}_{t-1} + V_t = R_t$.

Step 2 (Likelihood). While we still await the IOI-observed object (being ourselves at position c_{t-1}), we can already make a forecast about this object. That forecast will be conditioned by our previous forecast about c_t , and the observation equation that allows us to go from c_t to a forecast of o_t . Using Equation 2, we thus get (arrow 2): $o_t | c_t, o_{1:t-1} \sim N(F_t \hat{c}_{t-1}, R_t + W_t)$. The obtained mean denoted $F_t \hat{c}_{t-1}$ is our forecast about the IOI-observed o_t . The total variance Q_t will include the system variance, R_t , plus the variance due to observation, W_t , thus $R_t + W_t = Q_t$.

Next, our IOI-observed object becomes available (arrow 3) and now we can calculate the prediction error e_t as the difference between the forecast $F_t \hat{c}_{t-1}$, and the IOI-observation o_t . The prediction error is therefore $e_t = o_t - F_t \hat{c}_{t-1}$.

Step 3 (Posterior). We now have our observation and so we can look back (in the graph) to adapt the IOI-class on which we based our forecast and prediction error measurement. This step involves the core of the Bayesian inference (arrow 4), which we formulate here in terms of probabilities: $P(c_t|o_{1:t}) \propto P(o_t|c_t, o_{1:t-1})P(c_t, o_{1:t-1})$. In terms of the graphism, it results in a step where we go from the IOI-observed object back to the IOI-class: $c_t|o_{1:t} \sim N(\hat{c}_t, \check{c}_t)$, where $\hat{c}_t = \hat{c}_{t-1} + K_t e_t$ and $\check{c}_t = R_t - K_t R_t$. The mean of c_t , denoted \hat{c}_t is equal to the previous mean \hat{c}_{t-1} plus the observation error e_t , weighted. The weighting factor K_t is sometimes called the Kalman gain. It is a ratio of the system variance R_t with respect to the total variance Q_t (= system variance + observation variance). If the observation variance is small, then the effect of the error on the IOI-class is large. If the observation variance is large, the effect is small, and that will imply that a large difference between the expected IOI-observed object and the real IOI-observed object will have a small impact on the IOI-class. The variance of c_t , denoted \check{c}_t is based on the previous variance, weighted by the Kalman gain. The formulas for \hat{c}_t and \check{c}_t are standard for the evaluation of conditional Gaussian distributions (Bishop, 2006).

Once these three steps (four arrows in Figure 1) are taken, our updating of the IOI-class is finalized. We use this result about \hat{c}_t and \check{c}_t as the assumption for our next sample, to further continue the updating. As such, the Bayesian inference is made dynamic.

2.3.2. The multivariate approach, with regularization

The aforementioned state-space model applies to a multivariate model, with several IOI-class processes running at the same time. Thereby, the IOI-classes can be forced to obey the IOI-meter by adding a regularizing term to the state equation (Equation 1). That term will drive the time-related IOI-meter (or the ratio among IOI-class time series) towards the out-of-time IOI-meter. The regularization is defined as $x_t = (m - m_t) - \frac{1}{C} \sum_{c=1}^C (m - m_t)$, where m stands for the out-of-time IOI-meter, m_t stands for the time-related IOI-meter at time t , and C stands for the total number of IOI-classes in m . The time-related IOI-meter is obtained by taking the duration of the IOI-class objects at time t and subtracting the lowest value from these values (in log2dur). In fact, a fraction of x_t , defined by a parameter g , is added to the IOI-class so that it gradually drives the IOI-classes to the ideal out-of-time IOI-meter.

For example, assume that the three IOI-class durations at t are 8.5, 7, and 5.7 log2dur, respectively, and m is {3, 1, 0} (ratios in log2dur). Then m_t is {8.5, 7, 5.7} 5.7 = {2.8, 1.3, 0}, and $m - m_t$ is {3, 1, 0} - {2.8, 1.3, 0} = {.2, -.3, 0}, whose mean is -.03. So, x_t becomes {.17, -.33, -.03}. If, in our state equation, we would add this term to the IOI-class durations at t we would drive our IOI-class to: {8.5, 7, 5.7} + {.17, -.33, -.03} = {8.67, 6.67, 5.67}. The corresponding time-related IOI-meter has {3, 1, 0}, which we wanted. However, in our state equation, we will drive the IOI-class process incrementally to this goal, hence, we multiply with a control parameter g that depends on the sampling rate of the process. Given the fact that new IOI-observations constantly come in occasionally, the regularization will be constantly at work, slightly driving the IOI-class processes to the out-of-time IOI-meter.

3. Diagnostic

In this section, artificial data are created and used for testing the algorithm's behavior. First, we test smoothness (in a univariate setting), then the regularization of the IOI-classes (in a multivariate setting). See https://github.com/IPEM/BLlistener_supplementary_material for more details on the parameters used for simulation and testing. Using the scripts, all figures can be replicated and parameters can be changed.

3.1. Smoothness effects

Smoothness is a feature of the IOI-classes' constancy. Smoothness is co-defined by the system variance V_t and the observation variance W_t , and their ratio $r = V_t / W_t$ is overall indicative of smoothing. To test smoothing, we generated a sinusoidal signal consisting of 75 data points. Then we generated 75 random numbers using a normal distribution with zero mean and standard deviation of 15% of the y-value of the sinusoid. These numbers were then added to the sinusoidal signal and the resulting values served as duration values of IOI-observed objects. We transformed these values to milliseconds so that they could be used as input to the Bayesian listener algorithm (dots in Figure 2, left panels). The goal is to retrieve a sinusoid-like IOI-class time series from the IOI-observed objects, using different values for V_t and W_t .

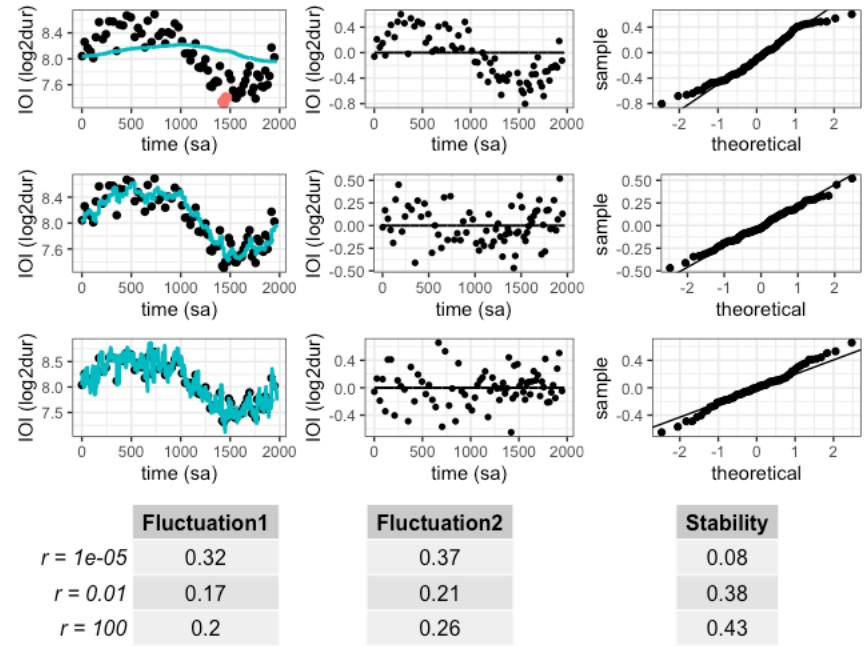


Figure 2. Smoothness effects. Different values for $r=V/W$ are shown in three rows of plots. The columns show the data and the retrieved IOI-class (log2dur over time in samples, 100 samples/second); the residuals (log2dur over time in samples), and the distribution (samples versus theoretical normal distribution, with -1 and 1 as standard deviation). The standard deviation of the residuals can be seen in the plot of the left column, on the y-value that corresponds to -1 or 1 on the x-axis. The rows of plots correspond with the rows in the table with $r=1e-4$, $r=0.01$, and $r = 100$.

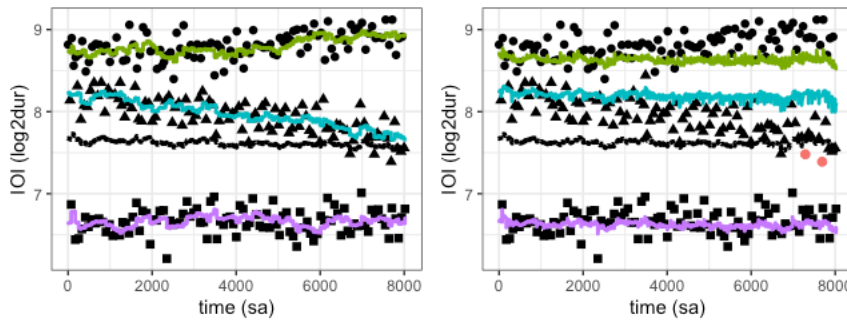
Figure 2 shows the effect for different ratios r in plots and tables. The first row of plots reveals a smooth curve (see the left panel) but the residuals lack a uniform distribution over time (see the middle panel) due to the fact that the curve has a delay, despite its normal distribution out-of-time (see the right panel). The second row of plots reveals a relatively

smooth curve with improved uniform distribution. The third row of plots reveals severe overfitting as the IOI-class jumps to each IOI-observed object with overshooting. The table shows the measured values for Fluctuation1, Fluctuation2, and Stability. The Fluctuation1 measure is based on the prediction error before Bayesian updating. After updating, the IOI-class will move to the IOI-observation but that brings it in a position that is away from the true mean and so the distance with another random IOI-observation is likely to be slightly larger than when the IOI-class would be positioned at the true mean. In addition, the algorithm is stochastic which means that noise is added to each observation. The second row with $r = 0.01$ and $W = 0.001$ and $V = 0.00001$ gives the best results for Fluctuation1 and Fluctuation2. Stability is just the standard deviation of the smoothed curve.

3.2. Regularization effects

In this section, we demonstrate the regularization effect with an artificial stimulus. As before we first define the IOI-classes and then we build IOI-observed objects that fluctuate around those IOI-classes. We work with three IOIs. IOI1 is going from 400 to 500 milliseconds, IOI2 goes from 300 to 200 milliseconds, and IOI3 remains constant at 100 milliseconds. Each have 100 data points, which we then translate to the $\log_2\text{dur}$ scale. Then, random numbers are generated at each data point, using a normal distribution with zero mean and standard deviation of $.15 \log_2\text{dur}$. When these random numbers are added to the IOI-classes, one obtains the IOI-observed objects, shown as dots in Figure 3. The next step, then, is the creation of a one-dimensional array of IOI-observed objects, by repeatedly taking values from the three IOI-classes. Finally, all values are translated to the millisecond scale. Accordingly, the first 6 first IOI-observed values are: 354, 321, 96, 472, 312, 100 milliseconds, and so on. The dataset thus simulates the situation that an ensemble plays in a meter which, while maintaining tempo, gradually shifts to another meter.

The task is to reconstruct the IOI-classes from the IOI-observed objects. The parameter g (see BLmain in the R-package BLlistener) thereby defines the strength of the regularization of the IOI-classes. Initial values are given as starting values for the IOI-classes, using an out-of-time meter indication of $\{4, 3, 1\}$ in milliseconds. The expected smallest IOI is 100 milliseconds. The left plot (Figure 3) shows that the IOI-classes capture the drift in the upper two IOIs. The right plot shows that the IOI-classes maintain the meter, despite the drift in the data. Due to regularization, the IOI-classes are forced to have a similar time-related IOI-meter and therefore, Fluctuation1 and 2 should increase for IOI1 and IOI2, as the prediction error becomes larger. The horizontal line around $7.6 \log_2\text{dur}$ is the IOI-tempo, which is derived from a linear combination of the IOI-classes, using the time-related IOI-meter as parameters. Often the goal is to plot tempo in the vicinity of about 2 Hz, which equals an IOI of 500 milliseconds, or about $9 \log_2\text{dur}$ (Van Noorden and Moelants, 1999). Given the relationship among the IOI-classes, the estimated tempo is very similar in both the non-regularized and the regularized analysis. In order to have a clear picture we plotted the IOI-tempo one $\log_2\text{dur}$ unit lower.



	g=0		
	F	F2	S
IOI1	0.13	0.16	0.09
IOI2	0.13	0.17	0.15
IOI3	0.13	0.17	0.06

	g=0.1		
	F	F2	S
IOI1	0.22	0.18	0.03
IOI2	0.28	0.21	0.04
IOI3	0.13	0.16	0.03

Figure 3. Regularization effect in plots and tables. Left plot: no regularization ($g = 0$). Right plot: with regularization ($g = 0.1$). The vertical axis is $\log_2 \text{dur}$ over time samples (100 samples/second). Dot-shapes (squares, triangles, circles) are IOI-observed objects that got assigned to the IOI-classes. The dotted line at about 7.6 $\log_2 \text{dur}$ indicates the tempo. $F1$ = Fluctuation1, $F2$ = Fluctuation2, and S = Stability.

4. Applications

In this section, we apply BListener to data from real music ensembles. The first example is a recording of student choir consisting of four singers. The second example is a re-analysis of a dataset consisting of 14 duet singers each performing 8 times the same song.

4.1. The MIT2019 dataset: trial 19

Figure 4 shows data from a choir of four singers (recorded in 2019 at Gent University). Here, we analyze one single performance, called "trial 19". The top plots of Figure 4 are based on a merging of individual recordings of each singer. These onset times were then concatenated, sorted and differentiated so that one single IOI sequence was obtained, which was then given as input to the BListener. The bottom plots of Figure 4 are based on an omni-microphone recording of the same performance. The parameters of the BLmain function are $\text{outt} = 1.5$, $tg = 360$, $\text{meter} = \{8,4,2,1\}$, $V = .00001$, $W = .001$. The JustHockIt data are contained in the R-package BListener. The script TestMIT2019ChoirTrial19.R to reproduce Figure 4 is available at https://github.com/IPeM/BListener_supplementary_material.

Due to asynchronization among singers, the merged recording shows many short IOIs. In the top left plot the analysis goes wrong because the lowest IOI-class drifts away and starts capturing those very short durations. In the top right plot, regularization is applied so that this drift doesn't happen and a rather decent pattern is obtained. In the bottom left plot, we see a random walk phenomenon in the upper two IOI-classes due to the fact that only few data are available. In the bottom right plot, regularization is applied and this reduces the variance

among IOI-class time series. The corresponding tables show global measures for each IOI-class.

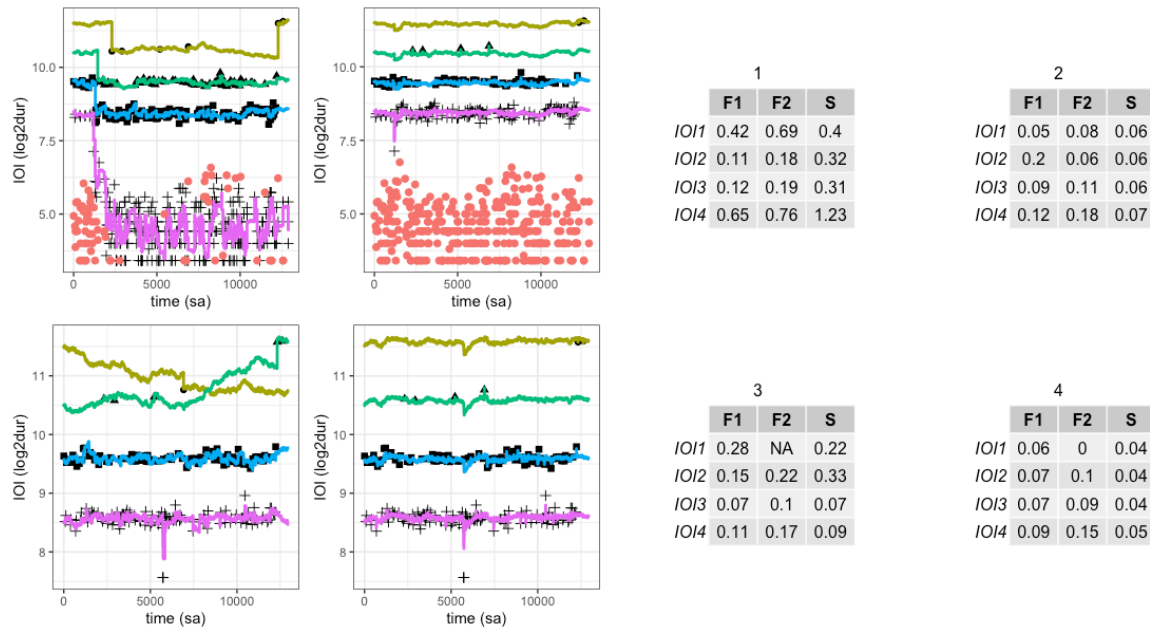
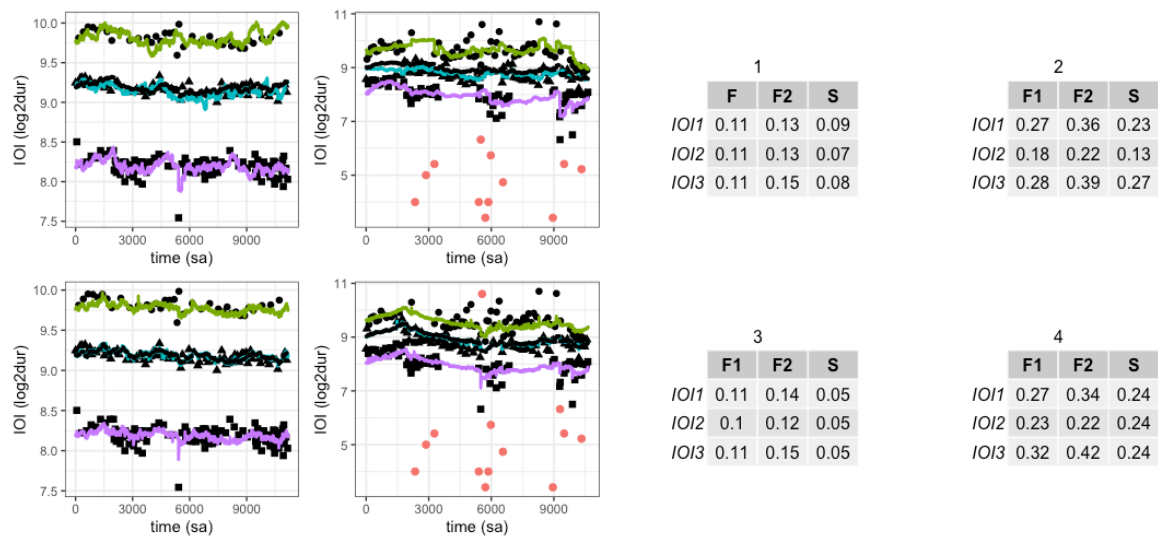


Figure 4. BListener applied to choir singing. The left plots have no regularization ($g = 0$), the right plots do have regularization ($g = .1$). The top plots have onset detection based on a merge of onsets extracted from the audio signals provided by four microphones. The bottom plots have onset detection based on a single audio signal provided by an omni-microphone recording. The tables show fluctuation and stability measures of IOI-classes. The labels "IOI1", "IOI2" etc. refer to the IOI-classes shown in the panels, starting from top to bottom. F1= Fluctuation1, F2 = Fluctuation2, S= Stability.

4.2. The JustHockIt dataset

The Bayesian listener algorithm is here applied to the JustHockIt dataset of duet singers (Dell' Anna et al., 2020). Our goal was to compare BListener results with previous reported findings. We used 14 human music ensembles plus 1 artificial MIDI reference from the JustHockIt dataset, each performing eight times the same song in two conditions, with movement (four trials) and without movement (four trials). The music ensembles consisted of two singers (duets), who alternately sang a note except for some short note repetitions. The parameters of the BLmain function are: $meter = \{3,2,1\}$, $outt = 1.5$, $V = 1e-05$, $W = 1e-03$, and either $g = 0$ or $g = 0.1$. The JustHockIt dataset is in the R-package BListener. A script TestJustHockIt.R to generate Figure 5, 6, 7 and 8 is available at https://github.com/IPeM/BListener_supplementary_material.



461
462

463 *Figure 5. Analysis of duets 16 and 4 from the JustHockIt dataset, in plots and tables. Left*
464 *plots show duet 16 and right plots show duet 4. Same for tables. The top row is without*
465 *regularization. The bottom row is with regularization. The horizontal axis in each plot shows*
466 *the time in samples (100 samples/seconds), the vertical axis shows duration in log2dur scale.*
467 *Each plot shows three horizontal lines representing the IOI-classes. The dotted horizontal*
468 *line (not always very visible due to overlap) represents the IOI-tempo. Big dots are outliers*
469 *but they appear only in the plots of duet 4. In tables, F1 is Fluctuation1, F2 is Fluctuation2, S*
470 *is Stability.*

471

472 Figure 5 shows an analysis of duet 16 and duet 4 without and with regularization. When the
473 music ensemble has its timing in agreement with the score, then the IOI-tempo (represented
474 by dotted lines) will fully overlap with the IOI-class (as in the plots of duet 16). However, for
475 expressive reasons, or for reasons that have to do with musical capabilities, it may happen
476 that a music ensemble's co-regulated timing slightly deviates from the prescribed meter in the
477 score, for example when short notes are performed shorter and long notes are performed
478 longer. Understanding how this timing elasticity relates to musical expressivity is a topic of
479 ongoing research (e.g., Coorevits et al., 2019). Here we see that duet 4 generates an IOI-
480 meter of about {3, 1.5, 1} (in milliseconds ratio) right from the beginning of the performance,
481 while the meter is in fact {3,2,1} (in milliseconds ratio). When regularization is applied, the
482 IOI-classes are forced to stay within the constraints of the out-of-time IOI-meter.

483

484 Figure 6 shows how narration reflects the structure of the music (as ABAB... scheme) in a
485 recurrence plot. Sequences of four labels holding IOI-class assignments (e.g., 1, 2, 1, 3) are
486 compared in a four-dimensional phase space, and at each time point this is done for past as
487 well as future time points. The comparison is either 1 or 0, depending on a threshold, and the
488 1s are represented as a dot. The recurrence ratio (RR) can be used as an additional mark of
489 homeostatic stability in co-regulated timing.

490

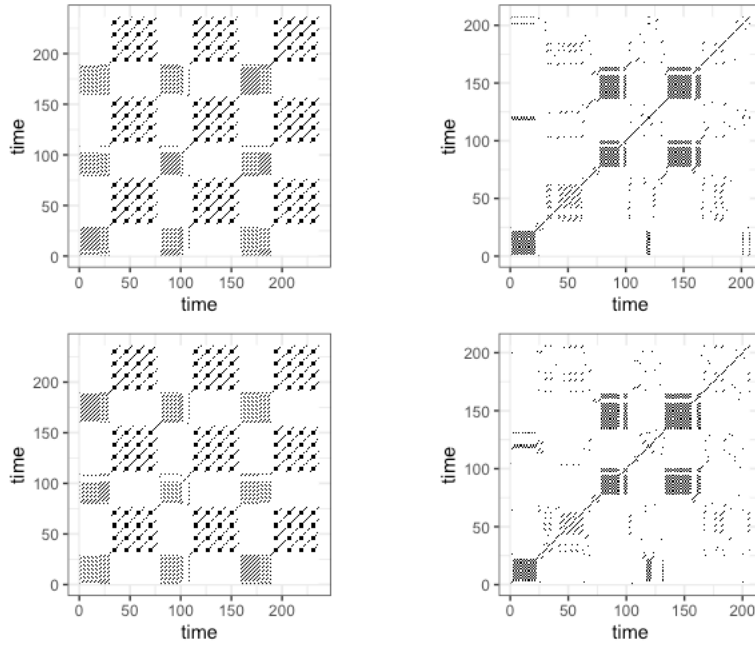


Figure 6. Recurrence plots of the plots in Figure 5. Time starts at the lower left corner and can be interpreted as going up to the upper right corner.

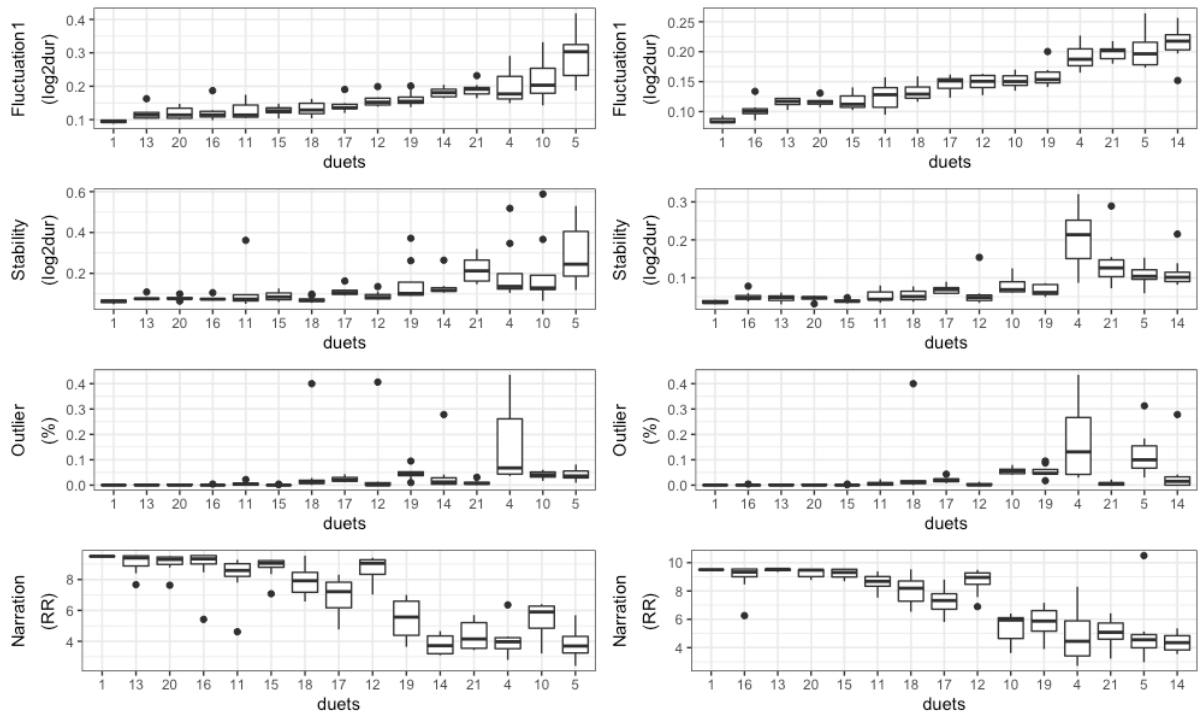


Figure 7. Comparison of global measures for the non-regularized ($g = 0$) (left column) and regularized ($g = .1$) (right column) analysis of the JustHockIt dataset. The horizontal axis in each panel shows the duets ordered according to the fluctuation1 per duet, as in the top plots¹. The bars show the mean and standard deviations for each measure. Conditions (movement, non-movement) are mixed as tests showed no distinction between moving and non-moving.

¹ Fluctuation1 calculates one value for each IOI-class. Rather than taking the mean over IOI-classes, we use only the fluctuation1 value of the second IOI-class.

Figure 7 provides an overview of the measures of the JustHockIt dataset. The duet numbers are labels, 15 in total. Duet 1 is a midi-based performance used here as control. Overall, the graph suggests that the measures are correlated, as summarized in Figure 8. Narration is reflecting the fact that low fluctuation implies more structure in the assignment of IOI-observed objects to IOI-classes.

Dell'Anna et al. (2020) also provides an assessment of performance quality and self-experienced agency, done by the performers themselves. Figure 7 gives an overview of the correlations of BListener measures (using Kendall's tau) and subjective estimates. The results are similar to the results of Dell'Anna et al. (2020).

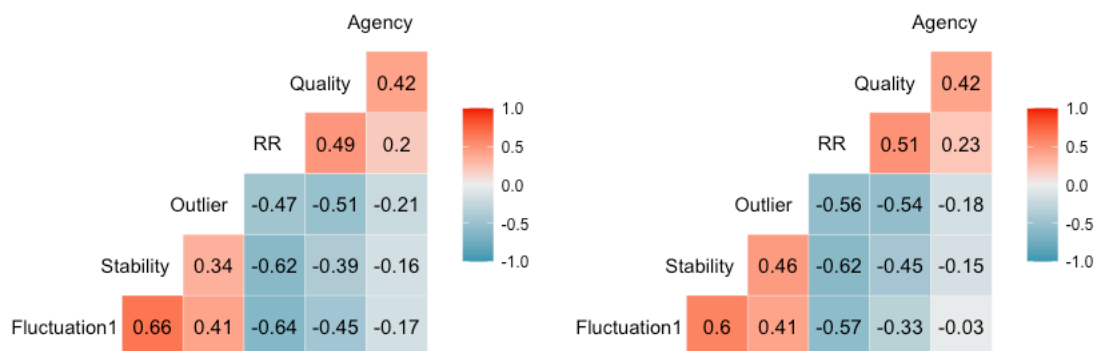


Figure 8. Correlation analysis of BListener measures (Fluctuation1, Stability, Outlier, Narration (or RR), all shown in Figure 7) with subjective measures (Quality, Agency). Without (left) and with (right) regularization.

The question whether regularization should be applied or not deserves caution, especially in relation to subjective self-assessments such as performance quality and agency. Regularization checks for the correct meter, and it discounts deviations from the assumed correct meter. However, it is possible that performers have a good impression of their own performance quality, as reflected in the annotation task and in the responses to agency questionnaires, despite the fact that the prescribed meter was not followed.

Discussion

From the viewpoint of the ensemble as a whole, the dynamics of co-regulated timing can be understood in terms of collaborative actions that bring about emergent patterns related to meter, rhythms, and tempo. From the viewpoint of a participating musician, the dynamics can be understood in terms of actions informed by hypotheses about the ensemble's overall timing. BListener is an attempt to model hypotheses formation using Bayesian inferencing. The outcome of BListener is a multivariate time series representing perceived timing constancy, given the music ensemble's co-regulated timing events (as inter-onset-intervals) as

input. From these time series it is possible to extract global features about the latent processes.

BListener has the option to regularize hypotheses about timing constancy by binding their variance. Thus, rather than assuming that the IOI-classes evolve independently from each other, we make them dependent using a hyper-parameter, which is the out-of-time IOI-meter. When regularization is turned on, BListener "believes" (weakly or strongly, depending on the control) that observed IOIs should be processed using the meter as prior. This regularization can be useful in contexts where obedience to the meter is regarded as a feature of the global timing intention. For example, the co-regulated timing of duet 10 in the JustHockIt database shows constancy but no adherence to the meter. A basic idea is that regularization also prevents drift of IOI-classes.

Constancy in timing correlates with the subjective assessment of timing quality and even with the subjective assessment of self-experienced agency (Dell'Anna et al., 2020). While statistical models can be built for predicting subjective experiences such as performance quality and agency, we restricted ourselves here to a simple correlation analysis which suggests that when timing becomes more predictive, the feeling of control becomes more pronounced. However, this finding needs further investigation since there are many confounding variables that play a role, such as level of musicianship and rehearsal time. Overall, it can be assumed that a music ensemble's capacity to establish timing constancy contributes to the resulting affective power on listeners, such as feelings of control or embodied synchronization. BListener thereby offers measures for timing constancy in non-stationary timing conditions such as expressive timing with rubato. However, further work is also needed here.

BListener focuses on perception rather than on action. However, by turning the BListener into a real-time algorithm equipped with musical synthesis tools it would be rather straightforward to set up computer simulations of co-regulated timing actions. A proof of concept was developed by Laghetto (2019) in a setting of three percussionists who jointly played a musical piece on percussion instruments. The algorithm's task was to track the timing constancy and provide feedback so that the musicians could adapt their timing in view of improving their co-regulation. The real-time application was based on the onset detector of the Python madmom package (Böck et al., 2012) and it used shifting averages of IOIs along the IOI-classes, as described in Dell'Anna et al. (2020). Colored lightening was used as feedback to measured fluctuation (which is used as marker of timing constancy, and for interaction quality), using variance levels as thresholds for different colors. The proof of concept showed that co-regulated timing can be traced and used as an indicator of interaction quality, which can be used in the feedback that drives the social interaction towards homeostatic regulation.

The current approach is embedded in the framework of dynamic linear models and state space representations thereof. However, the current implementation has some weak points. For example, BListener adopts a discrete approach to timing, as it takes onsets as input. But in some music, timing is based on amplitude modulations without strong energetic bursts, which is hard to perform onset detection. A next example concerns the dependency on priors. Although priors are considered a major strength of the Bayesian approach, their specification of priors can be hard and delicate. For example, when the IOI-classes are set to be highly adaptive to observations, their trajectory can go terribly wrong when certain priors are not properly set, as illustrated in Figure 4. Especially in view of real-world applications, more

work is needed to prepare for unexpected situations. In such contexts, it is likely that the regularization with the out-of-time IOI-meter needs more flexibility. Another possible point of improvement is the rather simple assignment rule of IOI-observations to IOI-classes, which is currently based on a difference between durations. This rule is blind for musical structure, since IOI-classes have no clue about narrative expectations. All these examples are illustrative of the fact that BListener is but a first step to a more encompassing solution.

Despite these and other limitations, BListener may be useful in applications involving music-based bio-feedback. Previous results in this domain (for example in Moens et al., 2014; Van den Berghe et al., 2020; Lorenzoni et al., 2019; Moumddjan et al., 2019; Buhmann et al., 2018) suggest that beneficial outcomes of human-machine synchronization are conditioned by constancy in co-regulated timing. If that parameter is of low quality, then beneficial effects will probably be poor or even neglectable, suggesting a dependency of effect on timing constancy. However, the timing of an interaction can be reinforced with bio-feedback. At this point, BListener can provide measures of co-regulation in social groups, which are useful in interactive multimedia systems that train synchronized social interaction skills in view of affective outcomes. In an application with fitness-machines (Fritz et al., 2015), it was shown that participants can co-regulate an ongoing audio stream using physical effort and concentration. The co-regulated activity can establish a particular interaction state that affects experiences of agency in participants. Similarly, research on individual-oriented music-based biofeedback systems shows that reinforcement learning can be used to steer users towards particular behaviors (e.g., Van den Berghe et al., 2020; Lorenzoni et al., 2019). BListener could be a component of a biofeedback system that uses reinforcement learning to steer users towards particular co-regulation behavior in view of attaining particular levels of timing constancy, and, likely, its associated performance quality.

Finally, it is important to realize that co-regulated timing in a music ensemble is more than Bayesian-inferencing. Co-regulated timing in a music ensemble is obviously intended, even before the music ensemble starts playing. Moreover, co-regulated timing is likely to involve states of affect and emotion such as feelings of agency and arousal, suggesting that Bayesian inferencing forms part of a more encompassing story. Earlier references to the concept of homeostasis pointed to a more encompassing dynamic of reward-based regulation and emotional states (Leman, 2016, pp. 188; Damasio, 2017). The metaphors reveal that humans are intrigued by extraordinary precarious states, especially when these states are difficult to self-realize.

Conclusion and future work

BListener is an algorithm that simulates how a listener-musician in a music ensemble captures the timing constancy of that ensemble, such that actions could be taken to co-regulate that timing. BListener only implements the perception part, not the action part. Currently, BListener can be applied to the off-line analysis of timing in music ensembles. BListener thereby operates in a discrete environment (using onsets). In future work, we also envision a real-time implementation of the algorithm, as perception component of an artificial musician who plays along with human musicians, capable of estimating timing constancy in human-machine interactions.

Supplementary Material

635 Scripts for generating and plotting all figures:
636 https://github.com/IPEM/BListener_supplementary_material
637
638 The R-package BListener can be found at <https://github.com/IPEM/BListener>
639

640 References

- 641 Aitchison, L. and Lengyel, M. (2017). With or without you: predictive coding and Bayesian
642 inference in the brain. *Current opinion in neurobiology*, 46, 219-227.
- 643 Agres, K., Abdallah, S. and Pearce, M. (2018). Information-theoretic properties of auditory
644 sequences dynamically influence expectation and memory. *Cognitive science*, 42(1), 43-76.
- 645 Bishop, C. (2006). *Pattern recognition and machine learning*. Berlin: Springer.
- 646 Bishop, L. (2018). Collaborative musical creativity: How ensembles coordinate spontaneity.
647 *Frontiers in psychology*, 9, 1285.
- 648 Bishop, L., Cancino-Chacón, C. and Goebel, W. (2019). Moving to communicate, moving to
649 interact: Patterns of body motion in musical duo performance. *Music perception*, 37(1), 1-25.
- 650 Bishop, L. and Goebel, W. (2020). Negotiating a shared interpretation during piano duo
651 performance. *Music and science*, 3, 2059204319896152.
- 652 Böck, S., Arzt, A., Krebs, F. and Schedl, M. (2012, September). Online real-time onset
653 detection with recurrent neural networks. In *Proceedings of the 15th International Conference*
654 *on Digital Audio Effects (DAFx-12)*, York, UK.
- 655 Buhmann, J., Moens, B., Van Dyck, E., Dotov, D. and Leman, M. (2018). Optimizing beat
656 synchronized running to music. *PLOS ONE*, 13(12).
- 657 Burger, B., London, J., Thompson, M. R. and Toiviainen, P. (2018). Synchronization to
658 metrical levels in music depends on low-frequency spectral components and tempo.
659 *Psychological research*, 82(6), 1195-1211.
- 660 Chang, A., Kragness, H., Livingstone, S., Bosnyak, D. and Trainor, L. (2019). Body sway
661 reflects joint emotional expression in music ensemble performance. *Scientific reports*, 9(1),
662 1-11.
- 663 Changeux, J-P. (1999). Leçon inaugurale, 16 janvier 1976, p.57. In A. Berthoz (Ed.) *Leçons*
664 *sur le corps, le cerveau et l'esprit*. Paris: Editions Odile Jacob.
- 665 Clarke, E. (1999). Rhythm and timing in music. In D. Deutsch (Ed.) *The psychology of*
666 *music* (pp. 473-500). Academic Press.
- 667 Cochrane, T., Fantini, B. and Scherer, K. (Eds.). (2013). *The emotional power of music:*
668 *Multidisciplinary perspectives on musical arousal, expression, and social control*. Oxford:
669 OUP.
- 670 Coorevits, E., Moelants, D., Maes, P-J. and Leman, M. (2019). Exploring the effect of tempo
671 changes on violinists' body movements. *Musicae scientiae*, 23(1), 87-110.

672 Damasio, A. (2017). *L'ordre étrange des choses: la vie, les sentiments et la fabrique de la*
673 *culture*. Paris: Odile Jacob.

674 D'Ausilio, A., Novembre, G., Fadiga, L. and Keller, P. (2015). What can music tell us about
675 social interaction? *Trends in cognitive science*, 19, 111-114.

676 Davies, K. (2016). Adaptive homeostasis. *Molecular aspects of medicine*, 49, 1-7.

677 Dell'Anna, A., Buhmann, J., Six, J., Maes, P. J. and Leman, M. (2020). Timing markers of
678 interaction quality during semi-hocket singing. *Frontiers in neuroscience*, 14.

679 Demos, A., Chaffin, R. and Kant, V. (2014). Toward a dynamical theory of body movement
680 in musical performance. *Frontiers in psychology*, 5, 477.

681 Fabian, D., Timmers, R. and Schubert, E. (Eds.). (2014). *Expressiveness in music*
682 *performance: Empirical approaches across styles and cultures*. Oxford: OUP.

683 Friston, K., FitzGerald, T., Rigoli, F., Schwartenbeck, P. and Pezzulo, G. (2017). Active
684 inference: a process theory. *Neural computation*, 29(1), 1-49.

685 Fritz, T., Hardikar, S., Demoucron, M., Niessen, M., Demey, M., Giot, O., Li, Y., Haynes, J.-
686 D., Villringer, A. and Leman, M. (2013). Musical agency reduces perceived exertion during
687 strenuous physical performance. *PNAS*, 110(44), 17784–17789.

688 Frühauf, J., Kopiez, R. and Platz, F. (2013). Music on the timing grid: The influence of
689 micro-timing on the perceived groove quality of a simple drum pattern performance. *Musicae*
690 *scientiae*, 17(2), 246-260.

691 Glowinski, D., Bracco, F., Chiorri, C. and Grandjean, D. (2016). Music ensemble as a
692 resilient system. Managing the unexpected through group interaction. *Frontiers in*
693 *psychology*, 7, 1548.

694 Glowinski, D., Bracco, F., Chiorri, C. and Grandjean, D. (2017). The resilience approach to
695 studying group interaction in music ensemble. In Lesaffre et al. (2017). *The Routledge*
696 *companion to embodied music interaction* (pp. 96-104). New York: Routledge.

697 Grimaud, A. M. and Eerola, T. (2020). EmoteControl: an interactive system for real-time
698 control of emotional expression in music. *Personal and ubiquitous computing*.
699 doi.org/10.1007/s00779-020-01390-7

700 Haken, H. (1990). Synergetics as a tool for the conceptualization and mathematization of
701 cognition and behaviour. How far can we go? In H. Haken and M. Stadler (Eds.) *Synergetics*
702 *of cognition*, (pp. 2-31) Berlin, Heidelberg: Springer.

703 Hilt, P.M., Badino, L., D'Ausilio, A., Volpe, G., Tokay, S., Fadiga, L. and Camurri, A.
704 (2019). Multi-layer adaptation of group coordination in musical ensembles. *Scientific reports*,
705 9(1), 1-10.

706 Kanai, R., Komura, Y., Shipp, S. and Friston, K. (2015). Cerebral hierarchies: predictive
707 processing, precision and the pulvinar. *Philosophical transactions of the royal society B:*
708 *biological sciences*, 370(1668), 20140169.

709 Keller, P. and Appel, M. (2010). Individual differences, auditory imagery, and the
710 coordination of body movements and sounds in musical ensembles. *Music perception*, 28(1),
711 27-46.

712 Keller P. (2014). Ensemble performance: interpersonal alignment of musical expression. In D
713 Fabian et al. (Eds). *Expressiveness in music performance: Empirical approaches across styles*
714 *and cultures*, pp. 260-282. Oxford: OUP.

715 Kelso, J. S. (1995). *Dynamic patterns: The self-organization of brain and behavior*.
716 Cambridge, MA: The MIT press.

717 Kotz, S. A., Ravignani, A. and Fitch, W. T. (2018). The evolution of rhythm processing.
718 *Trends in cognitive sciences*, 22(10), 896-910.

719 Laghetto, P. (2019). Time-evaluation model for live interaction with multiple performers.
720 MA-thesis at Padova University and Ghent University.

721 Leman, M. (2007). *Embodied music cognition and mediation technology*. Cambridge, MA:
722 The MIT press.

723 Leman, M. (2016). *The expressive moment: How interaction (with music) shapes human*
724 *empowerment*. Cambridge, MA: The MIT press.

725 Levitin, D. J., Grahn, J. A. and London, J. (2018). The psychology of music: Rhythm and
726 movement. *Annual review of psychology*, 69, 51-75.

727 London, J. (2012). *Hearing in time: Psychological aspects of musical meter*. Oxford: OUP.

728 Lorenzoni, V., Staley, J., Marchant, T., Onderdijk, K., Maes, P.-J. and Leman, M. (2019).
729 The sonic instructor: A music-based biofeedback system for improving weightlifting
730 technique. *PLOS ONE*, 14(8).

731 Moens, B., Muller, C., van Noorden, L., Franěk, M., Celie, B., Boone, J., Bourgois, J. and
732 Leman, M. (2014). Encouraging spontaneous synchronisation with D-Jogger, an adaptive
733 music player that aligns movement and music. *PLOS ONE*, 9(12).

734 Nakayama, S., R. Soman, V. and Porfiri, M. (2020). Musical collaboration in rhythmic
735 improvisation. *Entropy* 2020, 22, 233.

736 Meinhold, R. and Singpurwalla, N. (1983). Understanding the Kalman filter. *The American*
737 *statistician*, vol.37, no.2, 123-127.

738 Moumddjian, L., Moens, B., Vanzeir, E., De Klerck, B., Feys, P. and Leman, M. (2019). A
739 model of different cognitive processes during spontaneous and intentional coupling to music
740 in multiple sclerosis. *Annals of the New York academy of sciences*, 1445(1), 27–38.

741 Petris, G., Petrone, S. and Campagnoli, P. (2009). *Dynamic linear models with R*. New York:
742 Springer.

743 Pezzulo, G., Rigoli, F. and Friston, K. (2015). Active Inference, homeostatic regulation and
744 adaptive behavioural control. *Progress in neurobiology*, 134, 17-35.

- 745 Polak, R., London, J. and Jacoby, N. (2016). Both isochronous and non-isochronous metrical
746 subdivision afford precise and stable ensemble entrainment: A corpus study of Malian jembe
747 drumming. *Frontiers in neuroscience*, 10, 285
- 748 Port, R. and Van Gelder, T. (1995). *Mind as motion: Explorations in the dynamics of*
749 *cognition*. Cambridge, MA: The MIT press.
- 750 Ravignani, A. and Madison, G. (2017). The paradox of isochrony in the evolution of human
751 rhythm. *Frontiers in psychology*, 8, 1820.
- 752 Repp, B. and Su, Y. (2013). Sensorimotor synchronization: a review of recent research
753 (2006–2012). *Psychonomic bulletin & review*, 20(3), 403-452.
- 754 Schiavio, A., van der Schyff, D., Cespedes-Guevara, J. and Reybrouck, M. (2017). Enacting
755 musical emotions. *Sense-making, dynamic systems, and the embodied mind. Phenomenology*
756 *and the cognitive sciences*, 16(5), 785-809.
- 757 Scheurich, R., Pfordresher, P. and Palmer, C. (2020). Musical training enhances temporal
758 adaptation of auditory-motor synchronization. *Experimental brain research* 238, 81–92
759 (2020).
- 760 Shumway, R. and Stoffer, D. (2017). *Time series analysis and its applications: with R*
761 *examples*. New York: Springer.
- 762 Tolston, M. T., Funke, G. J., and Shockley, K. (2020). Comparison of cross-correlation and
763 joint-recurrence quantification analysis based methods for estimating coupling strength in
764 non-linear Systems. *Dynamics*, 29(31), 32.
- 765 Van den Berghe, P., Gosseries, M., Gerlo, J., Lenoir, M., Leman, M. and De Clercq, D.
766 (2020). Change-point detection of peak tibial acceleration in overground running retraining.
767 *Sensors*, 20, 17.
- 768 Van Nort, D. and Depalle, P. (2017). Adaptive musical control of time-frequency
769 representations. In R. Bader (Ed.). *Springer handbook of systematic musicology*. Berlin:
770 Springer, pp. 313-328.
- 771 Volpe, G., D'Ausilio, A., Badino, L., Camurri, A. and Fadiga, L. (2016). Measuring social
772 interaction in music ensembles. *Philosophical transactions of the royal society B: biological*
773 *sciences*, 371(1693), 20150377.
- 774 Vuust, P. and Witek, M. (2014). Rhythmic complexity and predictive coding: a novel
775 approach to modeling rhythm and meter perception in music. *Frontiers in psychology*, 5,
776 1111.
- 777 Witek, M., Clarke, E., Wallentin, M., Kringelbach, M. and Vuust, P. (2014) Syncopation,
778 body-movement and pleasure in groove music. *PLOS ONE* 9, e94446.